UC Merced

Title

Local Field Fluorescence Microscopy: Imaging Cellular Signals in Intact Hearts.

Permalink

https://escholarship.org/uc/item/9z7539ts

Authors

Aguilar-Sanchez, Yuriana
Fainstein, Diego
Mejia-Alvarez, Rafael
et al.

Publication Date

2017-03-01

DOI

10.3791/55202

Peer reviewed

Video Article

Local Field Fluorescence Microscopy: Imaging Cellular Signals in Intact Hearts

Yuriana Aguilar-Sanchez*[1], Diego Fainstein*[2,3], Rafael Mejia-Alvarez[4], Ariel L. Escobar[5]

[1]School of Natural Sciences, University of California, Merced

[2]Centro de Investigaciones Cardiovasculares, Universidad de la Plata and Conicet

[3]Facultad de Ingenieria, Universidad Nacional de Entre Rios

[4]Department of Physiology, Midwestern University

[5]School of Engineering, University of California, Merced

*These authors contributed equally

Correspondence to: Ariel L. Escobar at aescobar4@ucmerced.edu

Abstract

In the heart, molecular signaling studies are usually performed in isolated myocytes. However, many pathological situations such as ischemia and arrhythmias can only be fully understood at the whole organ level. Here, we present the spectroscopic technique of local field fluorescence microscopy (LFFM) that allows the measurement of cellular signals in the intact heart. The technique is based on a combination of a Langendorff perfused heart and optical fibers to record fluorescent signals. LFFM has various applications in the field of cardiovascular physiology to study the heart under normal and pathological conditions. Multiple cardiac variables can be monitored using different fluorescent indicators. These include cytosolic $[Ca^{2+}]$, intra-sarcoplasmic reticulum $[Ca^{2+}]$ and membrane potentials. The exogenous fluorescent probes are excited and the emitted fluorescence detected with three different arrangements of LFFM epifluorescence techniques presented in this paper. The central differences among these techniques are the type of light source used for excitation and on the way the excitation light is modulated. The pulsed LFFM (PLFFM) uses laser light pulses while continuous wave LFFM (CLFFM) uses continuous laser light for excitation. Finally, light-emitting diodes (LEDs) were used as a third light source. This non-coherent arrangement is called pulsed LED fluorescence microscopy (PLEDFM).

Video Link

The video component of this article can be found at https://www.jove.com/video/55202/

Introduction

The heart is the central organ of the cardiovascular system. The heart's contraction is initiated by an increase in intracellular $[Ca^{2+}]$. The relationship between electrical excitability and changes in intracellular Ca^{2+} release has been historically studied in enzymatically dissociated cells[1,2]. However, cardiac cells are electrically, metabolically and mechanically coupled[3,4]. When isolated, the myocytes are not only physically uncoupled, but myocytes from different layers are mixed during the dissociation[5]. Furthermore, despite the enormous advantages that have emerged from the study of isolated cells under voltage clamp conditions,[6,7,8] the intrinsic nature of the heart as an electrical syncytium always poses the question of how functionally different are dissociated cells from those present in the tissue[3].

In this manuscript, we describe the advances obtained in the knowledge of cardiac physiology by the use of local field fluorescence microscopy (LFFM) techniques in the intact heart. LFFM uses fluorescent indicators to measure multiple physiological variables such as cytosolic Ca^{2+}, intra sarcoplasmic reticulum (SR) Ca^{2+} and membrane potential. These measurements can be obtained simultaneously and in conjunction with ventricular pressure[9,10], electrocardiograms[9], electrical action potentials (APs), ionic current recordings and flash photolysis of caged compounds[4,11]. In addition, these measurements can be obtained by pacing the intact heart at higher frequencies closer to physiological rates. Although several articles[9,11,12,13,14] have been published by our group using LFFM techniques, the presumption of technical complexities associated with this technique has prevented its massive use in studying *ex vivo* physiological phenomena in the heart and other organs.

The LFFM technique (**Figure 1**) is based on epifluorescence measurements obtained using a multimode optical fiber in contact with the tissue. Like any contact fluorescence imaging technique, the optical resolution depends on the diameter and the numerical aperture (NA) of the fiber. A higher NA and smaller diameter of the fiber will increase the spatial resolution of the measurements. NAs and fiber diameters can range from 0.22 to 0.66 and from 50 μm to 1 mm, respectively. Increasing the NA will improve the signal to noise ratio (S/N) by accepting photons arriving from a larger solid angle. In order to act as an epifluorescence device, the light beam is focused into the optical fiber with an aspheric lens or an epifluorescence objective where the NA of the lens and the fiber match. This matching maximizes the energy transfer for excitation and for collecting back the photons emitted by the fluorophore.

In order to excite the exogenous fluorescent indicators loaded in the tissue, different light sources and illumination modes can be utilized. Our pioneering studies using the pulsed local field fluorescence microscopy[3,12] (PLFFM) employed a low-cost picosecond laser (**Figure 1a,** PLFFM). This type of light source has the huge advantage of exciting a big fraction of fluorophore molecules under the illumination area without substantially bleaching the dye due to the short pulse durations[12]. Additionally, the use of ultrashort pulses allowed the assessment of the fluorescence lifetime of the dye[12]. The fluorescence lifetime is a property that can be used to quantify the fraction of dye molecules bound to Ca^{2+}. Unfortunately, the temporal jittering of the pulses and variations in amplitude from pulse-to-pulse limit the application of this experimental strategy to cases where the change in fluorescence produced by the ligand binding to the dye is large.

Continuous Wave (CW) lasers are usually used as the main illumination source in LFFM (**Figure 1b,** CLFFM). The laser beam can continuously illuminate the tissue or can be ferroelectrically modulated. The ferroelectric modulation of the beam allows the generation of microsecond pulses of light. This modulation can be controlled by external hardware. This procedure not only dramatically reduces the temporal jittering of light pulses but also allows mixing beams of different wavelengths. The mixing of beams is done by multiplexing rays from different lasers. As a consequence, multiple dyes having different spectral properties can be excited to perform measurements of a variety of physiological variables, for example, Rhod-2 for cytosolic Ca^{2+}, MagFluo4 for intra-SR Ca^{2+} and di-8-ANEPPS for membrane potential.

Although lasers present various advantages as the light source in LFFM, other types of light sources can be used including light-emitting diodes (LEDs). In this case, the excitation light source consisted of an InGaN LED (**Figure 1c,** PLEDFM). In LEDs, photons are spontaneously emitted when electrons from the conduction band recombine with holes in the valence band. The difference with solid-state lasers is that the emission is not stimulated by other photons. This results in a non-coherent beam and a wider spectral emission for LEDs.

Different types of high power LEDs can be used. For AP recordings using Di-8-ANEPPS and for Ca^{2+} transients recorded using Fluo-4 or Mag-Fluo-4, we used an LED that has a typical peak emission at 485 nm (blue) and a half width of 20 nm (**Figure 1d**). For Ca^{2+} transients recorded with Rhod-2, the LED had a typical peak emission at 540 nm (green) and a half width of 35 nm (**Figure 1d**). LEDs emit in a band wavelength and therefore require filters to narrow their spectral emission. In addition, pulsed light can be generated at a rate of 1.6 kHz with duration of 20 µs. The LEDS were pulsed with a fast power MOSFET field effect transistor. Simultaneous recordings with different indicators can be performed by time-multiplexing the LEDs. Unfortunately, light emitted by LEDs is more difficult to focus onto a fiber optic compared to a laser beam. Thus, the main drawback of using LEDs is that their emission profiles have angular displacements (± 15°) from the main axis, and an auxiliary optic must be used to correct it.

In all of the optical configurations previously described, the excitation light is reflected with the aid of a dichroic mirror. The beam is subsequently focused by an aspheric lens and a microscope objective onto a multimode fiber optic that is positioned on the tissue. As in any epifluorescence arrangement, the dichroic mirror also serves to separate the excitation from the emitted light. The emitted light spectrum travels back through a barrier filter to remove any reflected excitation. Finally, the emitted light is focused with an objective onto a photodetector (**Figure 1**).

The transduction from light to electrical current is performed by silicon avalanche photodiodes. These diodes have a fast response and a high sensitivity allowing low light detection. The photocurrent produced by the avalanche photodiodes can be amplified in two ways: a transimpedance amplifier having a resistive feedback element (**Figure 1e**) or by an integrator to convert the current into a voltage (**Figure 1f**). Using the first approach, the output voltage is proportional to the photocurrent and the feedback resistor. A typical example of the resistive detection of picosecond laser pulses is shown in **Figures 2a, 2b** and **2c**. Panel **2a** illustrates the output of the transimpedance amplifier and panel **2b** shows a time expansion of the interval indicated with an asterisk (*). A peak tracking algorithm was implemented to detect the peak (red) and the base (green) for the fluorescent responses[12]. The measurement of the base fluorescence provides information of both the dark current of the avalanche photodiode and the interferences introduced by ambient light and electromagnetic coupling. A representation of peaks and bases is shown in **Figure 2c.** This figure illustrates the fluorescence emitted by the dye (Rhod-2) bound to Ca^{2+} during the cardiac cycle of a beating parakeet heart.

In the second method, the output voltage of the integrator is a function of the current and capacitive feedback (**Figures 2d, 2e,** and **2f**). **Figure 2f** shows two consecutive integration cycles: the first with no external illumination and the second with applied light pulses from a pulsed LED. A detailed description is presented in **Figures 2g** and **2h**. This approach, although more laborious, provides a larger S/N due to the absence of thermal noise in the feedback capacitor. The instrument includes a timing stage that generates all the control and multiplexing of the excitation light and commands the headstage integration and reset periods. This is usually performed with a digital signal processing circuit that also performs a digital differentiation of the integrated output signal by computing an *on-line* regression of the data. In the case of using a resistive feedback, any A/D acquisition board can be used.

Finally, our LFFM technique is highly versatile and can be adapted to record from more than one region. Adding a beam splitter in the light path allows us to split the light into two optical fibers. Each optical fiber can then be placed on different regions of a tissue to, independently, excite and record emission from the exogenous fluorescent probes. This modification permits us to assess how anatomical regional differences influence physiological variables. **Figure 3** shows a beam splitter being employed to split the CW excitation light such that two optical fibers are used to measure transmural electrical or intracellular $[Ca^{2+}]$ levels with minor-invasiveness. Transmural signals can be recorded by placing one fiber on the endocardium and the other on the epicardium layer of the ventricular wall. Therefore, the LFFM technique has the ability to measure the time course of cellular signals in different regions and can be used to test if regional changes occur under pathological situations.

Protocol

This protocol and all mice handling was approved by the UC Merced Institutional Animal Care and Use Committee (No. 2008-201). Experiments with parakeets were conducted in 1999 according to general policies for animal use established by the scientific commission of the Venezuelan Institute for Scientific Research (IVIC).

1. Langendorff Set Up Preparation

1. Prepare Tyrode solution containing the following solute concentrations in mM: 140 NaCl, 5.4 KCl, 2 CaCl$_2$, 1 MgCl$_2$, 0.33 Na$_2$HPO$_4$, 10 glucose, 10 HEPES. Adjust the pH of the Tyrode solution to 7.4 with NaOH and filter the solution through a 0.22 µm filter.
2. Load the Tyrode solution into the 60 mL syringes and all the tubing of the horizontal Langendorff set-up[11,12] illustrated in **Figure 4**. Make sure to eliminate all air bubbles.
3. **Equilibrate Tyrode solution with 100% O$_2$ using a submerged plastic "air stone" as illustrated in Figure 4.**
    1. Connect plastic tubing to an O$_2$ tank.
    2. Add a plastic Tee adapter to lower a 5" tube into the Tyrode solution in the 60 mL syringe.
    3. Attach a plastic air stone to the end of the 5" tube so O$_2$ will bubble out into the Tyrode solution.

4. Place a non-absorbable surgical suture around a needle used as a cannula. The needle is coupled to the manifold (see **Figure 4**) that allows retro-perfusion with different solutions. Finally, the heart's aorta will be cannulated into the needle.

2. Animal Preparation and Heart Dissection

1. Weigh and inject the mouse with heparin (ex. Mouse of weight 20 g, inject with 20 units or 200 µL) 15 min before euthanizing by cervical dislocation. Anesthetize parakeets according to the animal use guides of your IACUC protocol and then proceed with cervical dislocation. NOTE: Use 8 weeks old mice or 20 g parakeets.
2. **Remove the heart from the thoracic cavity after euthanization. Extract parakeet hearts in exactly the same way as described for mice.**
    1. Clean the mouse chest with ethanol.
    2. Using dissection scissors, make an incision in the lower abdomen and then cut up the sides toward the neck.
    3. Pull back the cut tissue and pin it down.
    4. Cut the diaphragm. Be careful when cutting the diaphragm to avoid damaging the heart.
    5. Remove the lungs and surrounding tissue.
    6. Use tweezers to scoop the heart without squeezing it. Cut the aorta as long as possible.

3. Transport the heart on a small weigh boat with approximately 1 mL Tyrode solution.
4. Using a non-absorbable surgical suture, tie the aorta onto the horizontal Langendorff apparatus via a needle. Tie the heart aorta with the aid of two fine tweezers. Begin retro-perfusion by opening the valve located in series with the 60 mL syringes containing Tyrode solution.
5. Allow the heart to stabilize for 10 min. Use this time to clean blood and the fatty tissue surrounding the heart before loading the dye. Pull the fatty tissue near the base of the heart with tweezers and cut using small dissection scissors. Be sure to do this under the view of a dissecting microscope.

3. Cytosolic Ca^{2+} Measurements: Preparing Dye Rhod-2AM

1. Add 20 µL of the 20% pluronic (a non-ionic surfactant) in DMSO to a special packaged plastic vial provided by the dye manufacturer containing 50 µg of the dye.
2. Mix by pipetting up and down, avoiding bubbles.
3. Transfer the mixed DMSO with the non-ionic surfactant and the dye from the special packaged plastic vial into a clear glass vial. Add 1 mL of Tyrode solution to the clear glass vial.
4. Sonicate for 15-20 min in a bath sonicator.
5. **Perfuse the dye using peristaltic pumps for 30 min at room temperature.**
    1. Place the dye in the dye chamber.
    2. Use a mechanical clamp to compress all the other tubing lines connected to the manifold. The clamp is placed above the manifold. This will prevent any backflow into the tubing connected to the 60 mL syringes.
    3. Turn on the perfusion peristaltic pump to begin circulating the dye. Immediately close the 3-way valve below the 60 mL syringe.
    4. Position a small tube that is connected to the suction peristaltic pump next to the heart to recirculate the dye that has been perfused into the heart.

4. Intra-SR Ca^{2+} Measurements: Preparing Dye Mag-Fluo4AM

1. Prepare Mag-Fluo4AM in the same manner as Rhod-2AM. Refer to section 3 for step-wise instructions.
2. After loading the dye, open the valve located in series with the 60 mL syringes containing Tyrode solution to begin retro-perfusion. Be sure to remove the clamp above the manifold.
3. Add Tyrode solution to the horizontal chamber and warm up to 37 °C.
4. Retro-perfuse with Tyrode solution for 45 min to remove the cytosolic dye.

5. Membrane Potential Measurements: Preparing Dye Di-8-ANEPPS

1. Add 5 mL of 99% ethanol to the dye vial that contains 5 mg of the dye.
2. Aliquot 10 µL into 500 individual 1 mL plastic vials using a repeater pipette.
3. Desiccate in a speed vacuum and store at -20 °C.
4. Add 20 µL of 20% pluronic in DMSO to a plastic vial with 10 µg of the desiccated dye.
5. Mix by pipetting up and down, avoiding bubbles.

6. Transfer the mix containing DMSO with pluronic and dye from the plastic vial to a graduated cylinder (10 mL). Add Tyrode solution to a final volume of 5 mL.
7. Sonicate for 20-25 min in a bath sonicator.
8. Perfuse into the heart for 30 min using peristaltic pumps. Refer to stepwise instructions in Section 3.5.

6 . Recording Epicardial Signals

1. After loading the dye, retro-perfuse the heart with Tyrode solution by removing the clamp above the manifold. Open the valve located in series with the 60 mL syringe containing Tyrode solution. Retro-perfuse Tyrode solution for 10 min to stabilize the heart.
2. Fill the horizontal chamber with Tyrode solution and turn on the peltier unit to bring the bath temperature to 37 °C.
3. **Position the fiber optic on the surface of the heart.**
    1. Place the fiber optic inside a 2 mL pipette and then attach the pipette to a micromanipulator.
    2. Use the micromanipulator to slightly press the fiber optic against the surface of the LV.

4. **Externally pace the heart with a stimulator controlled by a wave generator.**
    1. Program the wave generator to provide a square pulse with a width of 1 ms.
    2. Set the stimulator to be externally synchronized and connect the external input to the wave generator.
    3. To each output of the stimulator, connect a wire with an acupuncture needle soldered at the end.
    4. Place both acupuncture needles in the apex of the heart approximately 3 mm apart from each other.
    5. Only after the needles are placed in the tissue, turn on the output of the stimulator to prevent electric shock.

5. In the acquisition software, adjust acquisition frequency to 10 kHz.

7 . Recording Endocardial Signals

1. Refer to step 6.1 and 6.2 to stabilize the heart after loading the dye.
2. Using a sharp 23Ga point about the size of the fiber optic, make a small hole in the surface of the heart in the LV near the septum.
3. Place an intravitreal surgery sclerotomy adaptor to aid in positioning the first fiber optic into the endocardium using a micromanipulator.
4. Externally pace the heart. Refer to step 6.4.
5. In acquisition software, adjust acquisition frequency to 10 kHz.

Representative Results

AP and Ca^{2+} transients in endocardium and epicardium

In order to compare signals across the ventricular wall, one fiber optic is positioned in the endocardium and the other in the epicardium. Comparing the morphology of an AP recorded from the endocardium with one from the epicardium is the best way to assess the transmural function. The ventricular wall is highly heterogeneous and thus, the morphology of the APs are very different in these two regions. It is well known that the endocardium has less I_{to} than the epicardium[17,18,19]. The less I_{to} makes the repolarization of phase 1 slower in the endocardium[18,20]. **Figure 5b** shows a typical optical recording of the AP from the endocardium and the epicardium. To perform these recordings, mice hearts were loaded with the potentiometric dye di-8-ANEPPs and fluorescence was measured using the CLFFM technique. The morphology of the optically recorded AP, particularly in phase 1, shows a slower time course for the endocardium (Action Potential Duration (APD) 30 is 8.01 ms ± 2.5) in comparison to epicardium (3.4 ms ± 0.59) (**Figure 5b**). In general, the APD can be described as the time it takes the AP to repolarize a certain percentage including 30, 70 or 90 (**Figure 5a**). These traces have been normalized and shifted to have overlapping phase 0. When comparing the APDs (**Figure 5c**), we see that the endocardium and epicardium are significantly different during phase 1. Although these APs are fluorescence signals, they can be calibrated to a specific membrane potential by simultaneously measuring the AP with a sharp microelectrode filled with 3 M KCl[13].

In addition to membrane potential, exogenous fluorescent indicators can be used to monitor intracellular $[Ca^{2+}]$. Typically, we use Rhod-2AM to measure intracellular Ca^{2+} transients because of its high dynamic range and its ability to stay in the cytosol even at physiological temperatures. **Figure 6b** shows a typical recording of the intracellular Ca^{2+} transients in the endocardium and epicardium layer. These results have been partially published[15]. In order to compare regional differences in the intracellular $[Ca^{2+}]$ levels, the kinetics of the Ca^{2+} transients were assessed (**Figure 6a**). Overall, the analysis of the Ca^{2+} transient kinetics (**Figure 6c**) shows that the Ca^{2+} transients from the endocardium had significantly slower kinetics than those recorded from the epicardium.

Ca^{2+} dynamics in the SR lumen

In the heart, the rise and fall of intracellular [Ca^{2+}] levels are critical in defining many physiological variables including pressure, contractility, and action potential duration (APD). The previous section described our ability to measure the cytosolic Ca^{2+} transients. The Ca^{2+} released from the SR is largely responsible for the rise in intracellular cytosolic Ca^{2+}. Thus, for every rise in the intracellular Ca^{2+} there is a Ca^{2+} depletion in the SR. However, cytosolic Ca^{2+} transients are not solely due to SR Ca^{2+} release, but also include Ca^{2+} coming into the cell through the plasma membrane. Our lab[16] has been able to evaluate the SR Ca^{2+} content by the use of a fluorescent dye, Mag-Fluo-4AM. Although this dye is de-esterified in the myoplasm and the SR, the myocytes can extrude out the cytosolic fraction. This dye extrusion can be promoted by simply increasing the temperature to 37 °C. At this temperature, the cytosolic dye is removed by an ATP-binding cassette like membrane protein. Fortunately, this protein is not present in the SR membrane. Therefore, after increasing the temperature to 37 °C, the fluorescence recorded using the PLFFM technique is mostly a result of the Ca^{2+} binding to the dye within the SR. In order to test the specificity of the organelle measurement, a caffeine pulse was applied to stimulate Ca^{2+} release through RyR. It is possible to observe that the signal is indeed a result of the SR depletion (**Figure 7**). The caffeine induced SR Ca^{2+} release (**Figure 7a**) produce both, a decrease in diastolic level of Mag-Fluo-4 fluorescence (92 ± 0.05% (N = 4, P = 0.012)) and a decrease in the amplitude of Ca^{2+} transients (51 ± 0.21% (N = 4, P = 0.003))[16]. Intra SR traces recorded before and after the caffeine stimulus are represented downward in **Figure 7b-7d**. As time progresses from the caffeine stimulus, amplitude of the SR depletion is smaller. **Figure 7e** illustrates that SR depletion not only induces a decrease in the amplitude of the Ca^{2+} signal but also slows down the SR Ca^{2+} release process. The fluorescence trace in **Figure 7a** has been previously published[15].

Pulsed LED: Action potentials

In **Figure 5** we showed that Di-8-ANEPPS can report changes in the membrane potential when it's excited at 532 nm. Under this excitation condition, there is a decrease of the emitted fluorescence at wavelengths higher than 590 nm. Interestingly, when this potentiometric dye is excited close to its maximum excitation wavelength (~476 nm), the fluorescence emission of the dye shifts to lower wavelengths when the membrane depolarizes. Consequently, this spectral shift permits us to record the emitted fluorescence at two different wavelengths. This spectral property of Di-8-ANEPPS allows the rationing of the emitted fluorescence recorded at two different wavelengths, a feature that is usually of great value because the final computed recording will be independent of the dye concentration in the membrane. In order to take full advantage of the Di-8-ANEPPS spectral shift, we used pulsed LEDs as a light source. We used pulsed blue light to excite the fluorophore. Excitation was performed at 485 nm, close to the peak absorption wavelength of Di-8-ANEPPS (~476 nm). Acquisition in two different emission spectroscopic bands allows ratio formation and the ability to increase S/N and reject common mode noise like environmental light and motion artifact in contracting hearts where the mechanical uncoupler blebbistatin has not been used. This situation is very important for experimental conditions where both the mechanical activity of the heart and the kinetics of Ca^{2+} transients need to be measured simultaneously.

The timing diagram of the PLEDFM is illustrated in **Figure 8a**. The diagram includes the control logic for the integration and reset of the photodetection headstage, the on-off timing of the LED and the analog-to-digital conversion. During the time course of an AP, the fluorescence detected in the green wavelength band shows an increase in intensity while the fluorescence detected in the red band decreases. **Figure 8b** shows that the change of the fluorescence signal produced by the membrane depolarization moves in different directions. However, the motion artifact produced by the heart contraction is always oriented in the same direction, independent of the emission wavelength. As explained before, data of both channels (green and red) must be software-conditioned before calculating the ratio. The conditioning includes offset and gain corrections. The selection of offset and gain level corrections is not automatic. The user of the software has to select the variables to condition the traces before the ratio. The resulting ratio in panel 8b (**Figure 8**) shows that the artifact introduced by the myocardial movement has cancelled.

The relative change of di-8-ANEPPS fluorescence during an AP is usually very small (~8% per 100 mV). This di-8-ANEPPS fluorescence change is much smaller than the one produced by the Ca^{2+} binding to Rhod-2 (<200%). Thus, in order to increase the signal to noise ratio of di-8-ANEPPS, multiple recordings can be averaged.

Pulsed LED: Simultaneous recordings of Ca^{2+} and membrane potential

The last goal using this experimental approach consists in performing simultaneous recordings of Ca^{2+} transients and APs. Simultaneous recordings of multiple physiological signals require resolving technical difficulties related to different aspects of the system including: coupling the light source with the optical fiber, matching the absorption spectrum of the dye with the emission of the LEDs, designing the analog and digital electronic circuit to generate the timing and acquisition as well as the development of fast software to analyze data on-line.

In our study, the selection of dyes depended on their spectral characteristics. Flourophores used to measure diverse signals must absorb in different spectral bands. This condition is essential to distinguish between signal sources. Every time that an LED having a different wavelength is used to excite the tissue, the fluorescence detected corresponds to the signal related with the dye that absorbs in that wavelength. In this way, fluorescence emission coming from different dyes, but in the same wavelength band, can be distinguished by the time at which each one is excited.

Nevertheless, the crosstalk between dye spectrums cannot be fully avoided. This is because the spectral absorption characteristics of the dyes make them absorb light with wavelengths far from their peak absorption. In our experiments, crosstalk was produced in both ways: (1) Rhod-2 being excited by the blue LED, adding a Ca^{2+} signal to the red channel AP trace, and (2) Di-8-ANEPPS being excited by the green LED, which appears on the Ca^{2+} transient signal (**Figure 9f**). This crosstalk can be corrected on-line, as illustrated in **Figure 9**. The procedure works because the intruding signal is a small percentage of the signal that needs to be measured. Finally, using this type of algebraic processing of the fluorecence from the dyes allowed us to separate AP (**Figure 9d**) form Ca^{2+} transients (**Figure 9h**). A detailed outline of this processing is described in the figure legend. It is important to notice that all the Pulsed LED experiments were performed a 28 °C.
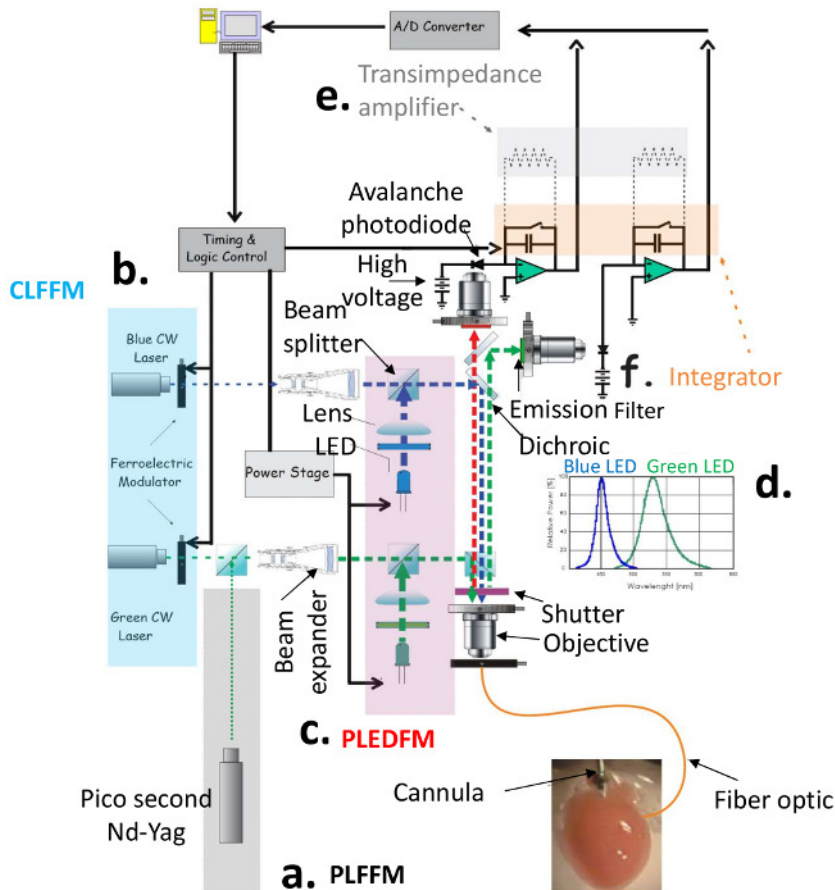
Figure 1: Local Field Fluorescence Microscopy (LFFM). The LFFM consists of an epifluorescence arrangement using a multimode optical fiber that is in contact with the tissue to record the fluorescence emitted from exogenous dyes perfused into the heart. The LFFM set-up can use three different light sources including (**a**) PLFFM, where excitation light is provided by a pulsed pico Nd-Yag laser; (**b**) CLFFM, where continuous wave lasers are used and light pulses are generated by a ferroelectric modulator allowing the multiplexing of lasers with different wavelengths; and (**c**) PLEDFM, where LEDs having broader emission spectrums with peak emissions of (**d**) 485 nm and 540 nm for blue and green LEDs, respectively, are electronically pulsed. When laser sources are used, the beam is defocused by a beam expander. Finally, dichroic mirrors and objective lenses focus the beam onto the fiber optic's distal end which is slightly pressed against the tissue. The emitted light travels back through the same fiber optic, dichroic mirror, emission filters, and is focused onto an avalanche photodiode where photons are converted into an electric current. The current can be amplified by two methods (**e**) transimpedance amplifier, where the resulting output voltage is proportional to the photocurrent and the feedback resistor; (**f**) integrator, where the output voltage is a function of the current and capacitive feedback. Finally, the signal is acquired by an A/D converter and viewed on a computer. Please click here to view a larger version of this figure.
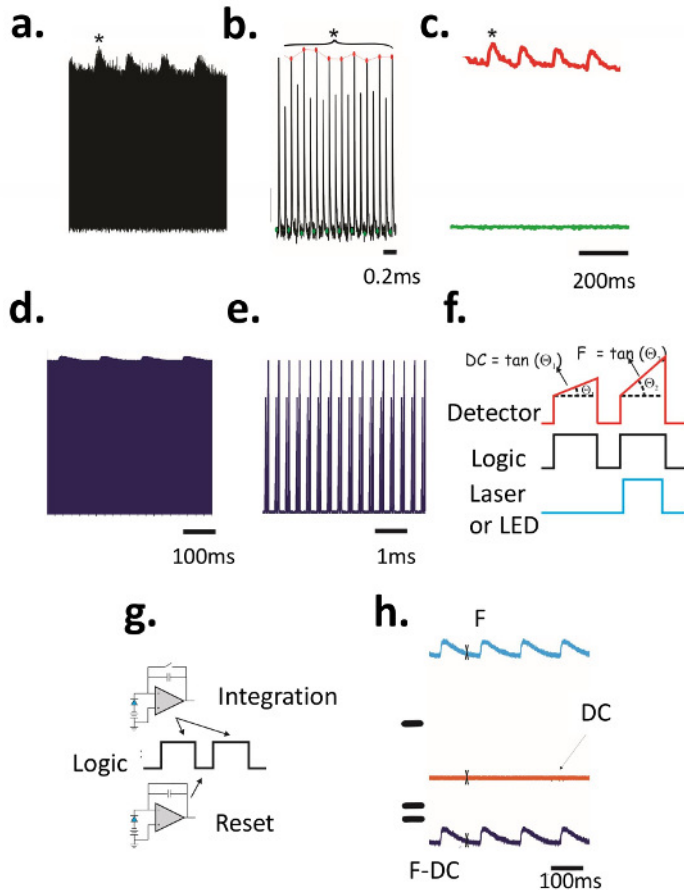
**Figure 2: Resistive and Capacitive Conversion.** (**a**) A typical example of the resistive detection of picosecond laser pulses is shown. The asterisk (**b**) shows a time expanded interval, where a peak tracking algorithm was implemented to detect the peak (red) and the base (green). (**c**) A representation of traces computed from peaks and bases recordings is shown for Rhod-2 fluorescent responses in a beating parakeet heart externally paced at 7 Hz and bath temperature set to 37 °C. **d to h**) The photocurrent converted by an integrator using a capacitive feedback. Typical recordings of intact mouse heart Ca^{2+} transients are shown in two different time scales (**d** and **e**). (**f**) The integration of two consecutive cycles with and without LED illumination are shown. The integral of the signal increases linearly as the photocurrent charges the feedback capacitor. The slope of the time dependent integral (tan (Θ)) is proportional to the number of photons impacting the avalanche junction in addition to the electron-hole recombination induced by the phononic activity when the avalanche diode does not detect any photons. The digital signals controlling headstage integration and reset periods are shown in panel **g**. Signals detected during the non-illuminating (DC) and LED illuminating period (F) are shown in panel **h**. The subtraction of F and DC provides the actual measurement of fluorescently detected Ca^{2+} transients from mice hearts externally paced at 9 Hz at 37 °C (**h**). Please click here to view a larger version of this figure.
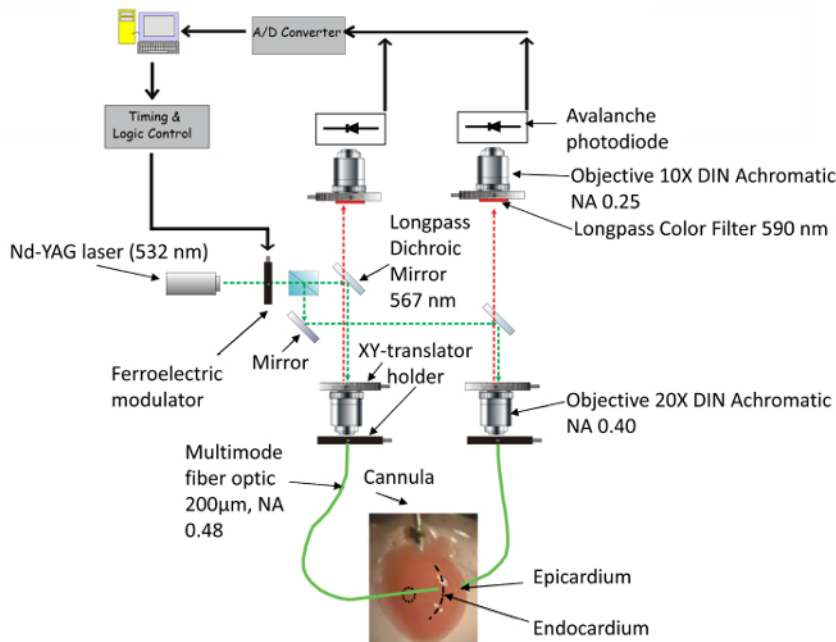
Figure 3: LFFM for Epicardium and Endocardium Measurements. The CLFFM set-up was used to measure the fluorescence emitted from exogenous fluorescent dyes present in the epicardium and endocardium layers. The addition of a beam splitter facilitated the recording of different physiological variables in the epicardium and endocardium. Two fiber optics were used with their individual headstages to detect from the epicardium and endocardium. A small circular incision was made in the ventricle and a fiber optic was threaded through to record from the endocardium. This set-up used a current-to-voltage converter with a resistive feedback. Please click here to view a larger version of this figure.
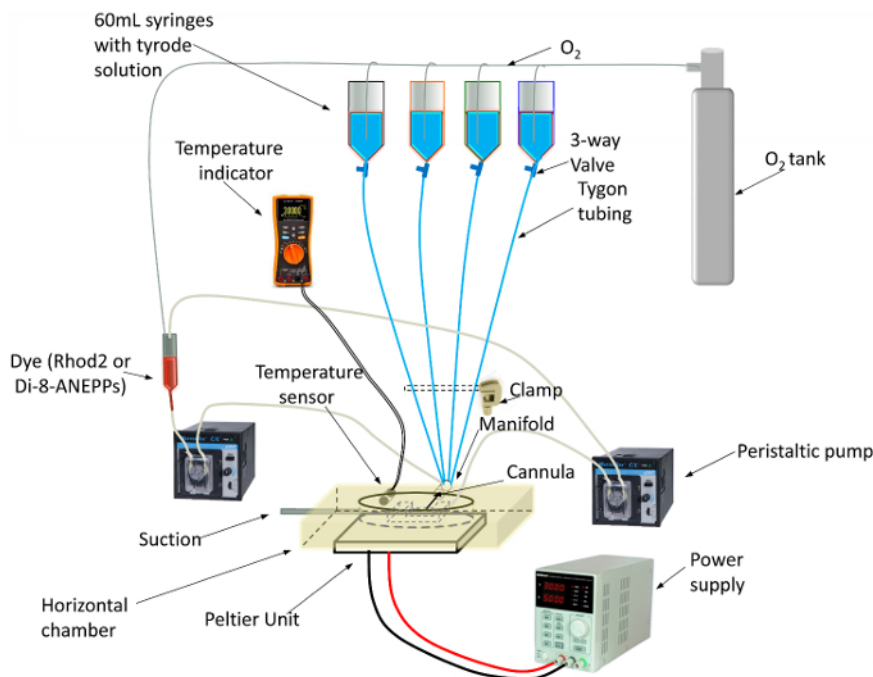

Figure 4: Horizontal Chamber with Temperature Control. A diagram showing the Langendorff set-up where intact hearts are maintained functional for hours. The heart is tied to a needle through which all solutions and dyes are retro-perfused into the heart via the coronaries branching off the aorta. The chamber is positioned above a peltier unit to maintain the temperature of the bath, which is read by a temperature sensor connected to a voltmeter. Please click here to view a larger version of this figure.

March 2017 | 121 | e55202 | Page 8 of 13
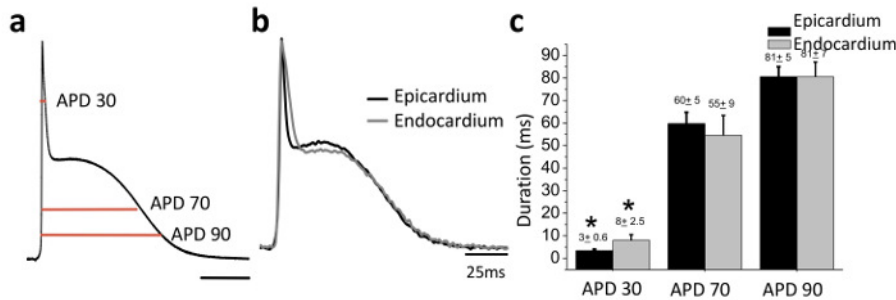
Figure 5: Transmural Action Potential Measurements in Intact Hearts. (**a**) Action potential duration (APD) is assessed as the time it takes to complete 30%, 70%, or 90% of the AP repolarization. (**b**) Di-8-ANEPPS fluorescence from the epicardium (black) and endocardium (grey) show AP morphological differences in repolarization between the two layers of the ventricular wall. (**c**) After assessing the APD 30, 70, and 90 in the endocardium and epicardium, results showed only significant differences occurred in APD 30 (8 ± 2.5 ms endocardium vs 3 ± 0.6 ms epicardium). Hearts were paced at 6 Hz and temperature set to 37 °C. Data are mean ± SEM of 5 hearts. *P <0.05. Please click here to view a larger version of this figure.
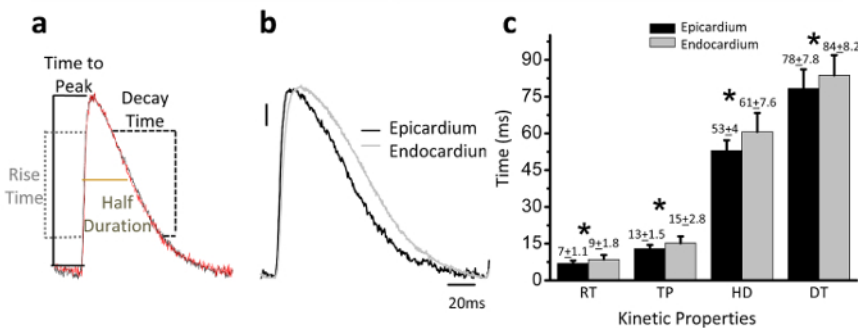

Figure 6: Transmural Ca^{2+} Transient Measurements in Intact Hearts. (**a**) Parameters of Ca^{2+} transient kinetics measured are: the time it takes to reach maximum, time to peak (TP); the time it takes to go from 10% to 90% of the rise, rise time (RT); the time it takes to go from 10% to 90% of the decay, decay time (DT); and the time it takes to complete 50% of the transient, half duration (HD). (**b**) Fluorescence emitted by Rhod 2 after excitation with a green CW laser show epicardium (black) and endocardium (grey) Ca^{2+} transients with differences in relaxation. **c**) Ca^{2+} transients from the endocardium had significantly slower kinetics in RT, TP, HD, and DT than those recorded from the epicardium. Hearts were paced at 6 Hz and temperature set to 37 °C. Data are mean ± SEM of 5 hearts. *P <0.05. Modified from Mattiazzi *et al.*[15]. Please click here to view a larger version of this figure.
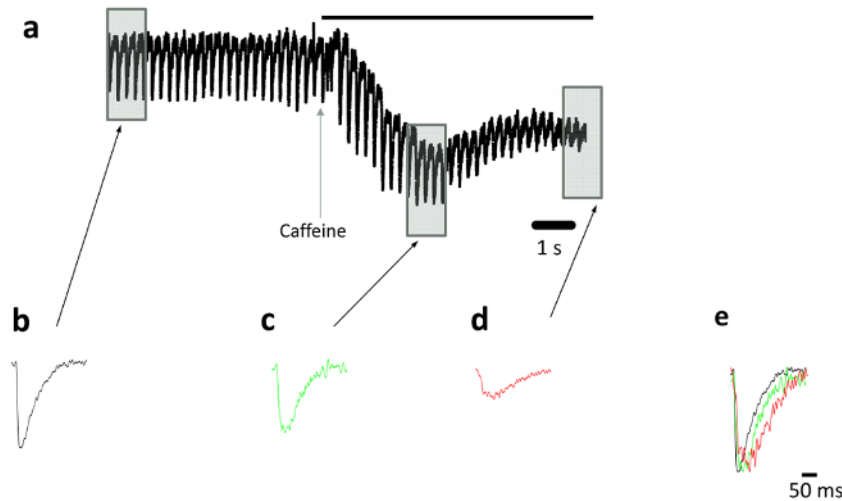
Figure 7: Intra SR Ca^{2+} Measurements in Intact Hearts. (**a**) The emitted fluorescence from the Mag-Fluo-4 dye drops over time, reflecting a decrease in the intra SR Ca^{2+} concentration. (**b**) The expanded view of the decrease in Mag-Fluo 4 fluorescence indicating Ca^{2+} depletion induced by Ca^{2+} release from the SR. (**c**) An expanded view of the decrease in transient amplitude from Mag-Fluo 4 fluorescence representing Ca^{2+} release modified by perfusing hearts with 20 mM caffeine. (**d**) After a long application of caffeine, a decrease in both the diastolic level of Mag-Fluo-4 fluorescence and in the amplitude of Ca^{2+} transients [down to $92 \pm 0.05\%$ (N = 4, P = 0.012) and $51 \pm 0.21\%$ (N = 4, P = 0.003) of initial values, respectively], is observed. As more time progresses from the caffeine, the smaller is the amplitude of the SR depletion. (**e**) Normalized traces in b-d shows that SR depletion not only induces decreases of the Ca^{2+} signal but also slows down SR Ca^{2+} replenishment. Hearts were paced at 4 Hz and temperature set to 37 °C. Fluorescence trace is from Kornyeyev *et al.*[16]. Please click here to view a larger version of this figure.
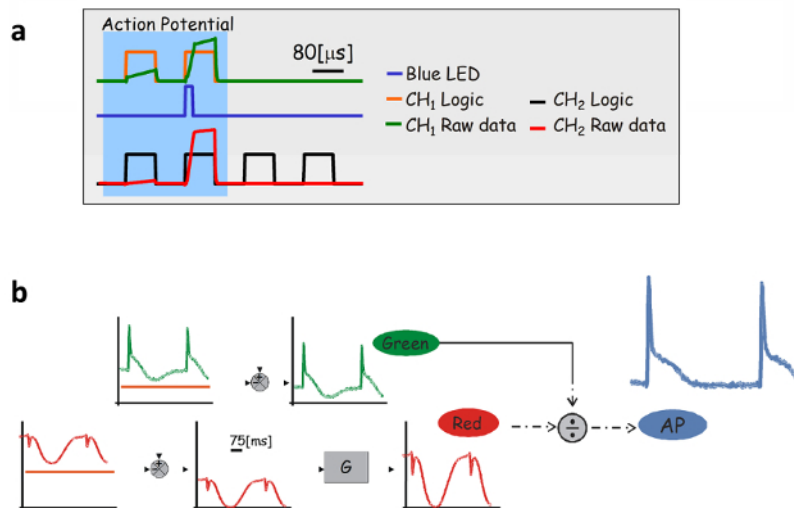
Figure 8: Ratiometric Measurements of APs in Intact hearts with Pulsed LED. (**a**) The timing diagram including integration and reset of the headstage, on-off times of the LED and an actual recording is illustrated. (**b**) Traces from the two channels have different resting values and the offset is corrected by moving the levers until each AP is preceded by a resting value. Gain of each channel is also adjusted. Note that a very big motion artifact appears on both channels between the two depolarizations. After the software processes the signals ratiometrically, the result is an AP without noticeable artifacts (blue). Hearts were paced at 3 Hz and temperature set to 28 °C. All the records shown are an average of 10 traces. Please click here to view a larger version of this figure.
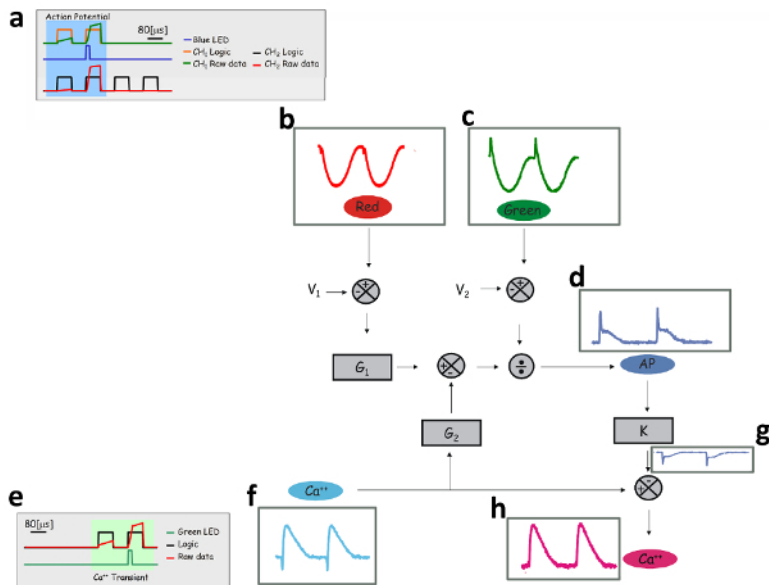
Figure 9: Simultaneous Ca^{2+} Transients and AP Measurements in Intact Hearts with Pulsed LED. The cross talk contamination of signals when recording both Ca^{2+} and AP can be corrected on-line. The potentiometric dye, di-8-ANEPPS, is excited with 20 µs blue LED pulses (**a**). Signals are split, filtered with bandpass red and green filters. These signals are detected by two different avalanche photodiodes indicated as the red (**b**) and green channel (**c**). It is possible to observe that both signals, red and green, present a noticeable movement artifact that appears as a downward deflection. Both signals, red and green, are offseted and then amplified. The conditioned signals are used to calculate the ratio between them and the result is shown in **d**. It is possible to observe that in the ratio between both signals (**d**) the moving artifacts are cancelled. Panel **e** illustrates the sequence of logic pulses that control a green emitting LED used to excite the Ca^{2+} indicator Rhod-2. Fluorescent signals obtained using this procedure are shown in **f**. Although the trace in **f** mostly shows an increase in the fluorescence signal due to the Ca^{2+} binding to Rhod-2, it is also possible to observe a negative deflection in the trace due to a fluorescently detected signal from Di-8-ANEPPS when this dye is excited with green light. This problem can be corrected by subtracting the potentiometric signal shown in **g**. The result of the subtraction is shown in panel **h** where a Ca^{2+} signal free of an AP contamination is obtained. Hearts were paced at 3 Hz and temperature set to 28 °C. All the records shown are an average of 10 traces. Please click here to view a larger version of this figure.

Discussion

This paper is centered in describing local field fluorescence techniques to evaluate the function of cardiac myocytes *ex vivo*. The study of these cells in a coupled environment is not only more physiological, but is also highly appropriate for assessing organ-level pathologies. The cellular events underlying excitation-contraction coupling (ECC) can be evaluated at the whole organ level with the use of molecular probes that monitor intracellular Ca^{2+} dynamics (Rhod 2 cytosolic Ca^{2+}, Mag-Fluo4 SR Ca^{2+}) and electrical activity (di-8-ANEPPs). Here, we have presented three LFFM epifluorescence techniques that both excite and collect the emission from fluorescent indicators using optical fibers. They differ based on the light source used and the type of light modulation. The PLFFM uses a laser that pulses light, CLFFM uses continuous laser light, while LEDFM uses LEDs that can also be pulsed in the PLEDFM. All of these are presented in **Figure 1** as one set, but can be constructed with only one of the three epifluorescence arrangements. In addition, the detected light can be processed in different ways. For example, **Figure 2** illustrates two different situations in which the photocurrent can be either integrated or directly converted to a voltage by means of a current-to-voltage converter. In general, the LFFM approach can be used to simultaneously measure multiple anatomical sites, as seen for **Figure 3.**

The method presented here for assessing cardiac properties at the intact organ level is more adequate to study problems in which the coupling between cells is critical in defining the behavior of the tissue. The intrinsic heterogeneity of the heart can produce different AP waveforms[13,21,22] based on the specific tissue from which cells originate. Therefore, whole organ studies provide the opportunity to assess the local physiological function of the cell in different anatomical structures. Moreover, we have seen that intracellular events like sparks and waves have different kinetics in dissociated cells than in the intact organ[15].

The Langendorff set-up (**Figure 4**) is critical in maintaining the heart in a situation that is closer to *in vivo*. Additionally, it allows the retroperfusion of multiple drugs and various fluorescent molecular probes that allow the measurement of several physiological variables. Changing the exogenous fluorescent probes used, increasing the size of the fiber optic, or choosing a different light source can dramatically alter the application of the technique. Additionally, the peltier unit below the horizontal chamber can facilitate the study of Ca^{2+} dynamics at various temperatures. Adding accessories to LFFM such as a beamsplitter can increase the number of fiber optics used to record from different regions in the intact heart. This is a very useful adaptation to test if regional differences occur in pathological scenarios. **Figure 3** shows the endocardium and epicardium being assessed simultaneously. Furthermore, perfusing the heart with different agonists allows us to understand how the different regions across the ventricular wall are regulated. The electrical signaling (**Figure 5**) and Ca^{2+} kinetic (**Figure 6**) heterogeneities can be compared at the epicardium and endocardium. In addition, multiple dyes with different excitation wavelengths and emission filters can be used. For example, by using Mag-Fluo-4, Ca^{2+} levels in the lumen of the SR can be recorded (**Figure 7**). Varying the size of the fiber optic can also extend the capacity of this method by allowing the fluorescent recording from a larger region.

This paper also shows that aside from expensive lasers, LEDs can be used as an excitation light source in our technique. **Figure 8** shows that this inexpensive type of light source can be used to ratiometrically measure APs. The ratiometric measurement shown in **Figure 8** is advantageous in producing a final recording without experimental artifacts including those caused by movement. Finally, even the Ca^{2+} transient and AP can be optically recorded, simultaneously, by multiplexing different wavelengths and using dyes with the same emission spectra. The processing of signals outlined in **Figure 9** is critical in removing internal contamination produced by the overlap in emission spectra of the dyes. Recording Ca^{2+} transients and APs, simultaneously, but as two independent output signals is beneficial in studying ECC and Ca^{2+}-induced Ca^{2+} release (CICR) which are processes where these two variables are highly interconnected.

LFFM is a technique with multiple applications in cellular physiology of intact tissues. However, one major limitation is that the recorded fluorescence is an average of the emission from the underlying fluorescent indicators in the local region where the optical fiber is in contact with the tissue. Even when using two fiber optics, LFFM does not provide a subcellular spatial distribution of the measured signals. Optical mapping is a better technique for monitoring physiological variables that change in space and time such as the propagation of the AP, Ca^{2+} transients, and alternans[23,24,25]. LFFM is also unable to provide imaging of structures, like confocal microscopy and other optical mapping techniques. Nevertheless, its use of fiber optics makes it practical in recording local fluorescence signals from the endocardium or other regions that are difficult or impossible to access in an intact heart with a confocal microscope.

The comparison between physiological variables obtained from intact hearts and from isolated myocyte experiments is challenging. The greatest advantage of using isolated cardiac myocytes is the unique opportunity to evaluate biophysical properties of the cells under patch clamp conditions. In contrast, LFFM allows the study of physiological and pathological phenomenon in a more native environment. For example, in intact hearts we can assess transmural differences[15], heart rate dependency of AP and Ca^{2+} at physiological ranges[13] that are unattainable in isolated cells. In addition, we can study the effects of an ischemic insult on the function of the intact heart[9,10]. Whole heart experiments also allow us to evaluate the interaction between other cell types and myocytes[11].

LFFM allows the visualization of cellular signals at the intact heart level in which cells have physiological coupling. LFFM allows the study of intracellular activity while cells are still in the intact organ. In combination with fluorescent dyes and epiluminescence, LFFM can monitor two key cardiac properties: Ca^{2+} dynamics and electrical activity.

Finally, the method presented here can have multiple applications in the study of ECC. It is a tool that reveals how supramolecular signals are affected in pathological situations such as arrhythmias[16] and ischemia[9,15]. This technique is a must to study these pathologies since they can only be understood at the intact organ level.

Disclosures

The authors have nothing to disclose.

Acknowledgements

References

1. Fabiato, A., & Fabiato, F. Contractions induced by a calcium-triggered release of calcium from the sarcoplasmic reticulum of single skinned cardiac cells. *J Physiol.* **249** (3), 469-495 (1975).
2. Mitra, R., & Morad, M. A uniform enzymatic method for dissociation of myocytes from hearts and stomachs of vertebrates. *Am J Physiol.* **249** (5), 1056-1060 (1985).
3. Escobar, A. L., et al. Developmental changes of intracellular Ca2+ transients in beating rat hearts. *Am J Physiol Heart Circ Physiol.* **286** (3), H971-978 (2004).
4. Ramos-Franco, J., Aguilar-Sanchez, Y., & Escobar, A. L. Intact Heart Loose Patch Photolysis Reveals Ionic Current Kinetics During Ventricular Action Potentials. *Circ Res.* **118** (2), 203-215 (2016).
5. Mitra, R., & Morad, M. A uniform enzymatic method for dissociation of myocytes from hearts and stomachs of vertebrates. *Am J Physiol.* **249** (5 Pt 2), H1056-1060 (1985).
6. Fischmeister, R., DeFelice, L. J., Ayer, R. K., Levi, R., & DeHaan, R. L. Channel currents during spontaneous action potentials in embryonic chick heart cells. The action potential patch clamp. *Biophys J.* **46** (2), 267-271 (1984).
7. Banyasz, T., Horvath, B., Jian, Z., Izu, L. T., & Chen-Izu, Y. Profile of L-type Ca(2+) current and Na(+)/Ca(2+) exchange current during cardiac action potential in ventricular myocytes. *Heart Rhythm .* **9** (1), 134-142 (2012).
8. Apkon, M., & Nerbonne, J. M. Characterization of two distinct depolarization-activated K+ currents in isolated adult rat ventricular myocytes. *J Gen Physiol.* **97** (5), 973-1011 (1991).
9. Valverde, C. A., et al. Transient Ca2+ depletion of the sarcoplasmic reticulum at the onset of reperfusion. *Cardiovasc Res.* **85** (4), 671-680 (2010).
10. Valverde, C. A., et al. Phospholamban phosphorylation sites enhance the recovery of intracellular Ca2+ after perfusion arrest in isolated, perfused mouse heart. *Cardiovasc Res.* **70** (2), 335-345 (2006).
11. Escobar, A. L., *et al.* Role of inositol 1,4,5-trisphosphate in the regulation of ventricular Ca(2+) signaling in intact mouse heart. *J Mol Cell Cardiol.* **53** (6), 768-779 (2012).
12. Mejía-Alvarez, R., *et al.* Pulsed local-field fluorescence microscopy: a new approach for measuring cellular signals in the beating heart. *Pflügers Arch.* **445** (6), 747-758 (2003).
13. Ferreiro, M., Petrosky, A. D., & Escobar, A. L. Intracellular Ca2+ release underlies the development of phase 2 in mouse ventricular action potentials. *Am J Physiol Heart Circ Physiol.* **302** (5), H1160-1172 (2012).

14. Kornyeyev, D., et al. Calsequestrin 2 deletion shortens the refractoriness of Ca^{2+} release and reduces rate-dependent Ca^{2+}-alternans in intact mouse hearts. *J Mol Cell Cardiol .* **52** (1), 21-31 (2012).

15. Mattiazzi, A., Argenziano, M., Aguilar-Sanchez, Y., Mazzocchi, G., & Escobar, A. L. Ca2+ Sparks and Ca2+ waves are the subcellular events underlying Ca2+ overload during ischemia and reperfusion in perfused intact hearts. *J Mol Cell Cardiol.* **79**, 69-78 (2015).

16. Kornyeyev, D., Reyes, M., & Escobar, A. L. Luminal Ca(2+) content regulates intracellular Ca(2+) release in subepicardial myocytes of intact beating mouse hearts: effect of exogenous buffers. *Am J Physiol Heart Circ Physiol .* **298** (6), H2138-2153 (2010).

17. Wang, Z. G., Fermini, B., & Nattel, S. Repolarization differences between guinea pig atrial endocardium and epicardium: evidence for a role of Ito. *Am J Physiol .* **260** (5 Pt 2), H1501-1506 (1991).

18. Liu, D. W., Gintant, G. A., & Antzelevitch, C. Ionic bases for electrophysiological distinctions among epicardial, midmyocardial, and endocardial myocytes from the free wall of the canine left ventricle. *Circ Res.* **72** (3), 671-687 (1993).

19. Litovsky, S. H., & Antzelevitch, C. Transient outward current prominent in canine ventricular epicardium but not endocardium. *Circ Res.* **62** (1), 116-126 (1988).

20. Lukas, A. Electrophysiology of Myocardial Cells in the Epicardial, Midmyocardial, and Endocardial Layers of the Ventricle. *J Cardiovasc Pharmacol Ther .* **2** (1), 61-72 (1997).

21. Antzelevitch, C., & Fish, J. Electrical heterogeneity within the ventricular wall. *Basic Res Cardiol.* **96** (6), 517-527 (2001).

22. Gómez, A. M., et al. Modulation of electrical heterogeneity by compensated hypertrophy in rat left ventricle. *Am J Physiol .* **272** (3 Pt 2), H1078-1086 (1997).

23. Efimov, IR. Innovation in optical imaging: looking inside the heart. *Heart Rhythm .* **4** (7), 925-926 (2007).

24. Boukens, BJ., Efimov, IR. A century of optocardiography. *IEEE Rev Biomed Eng .* **7**, 115-125 (2014).

25. Zhang, H., Iijima, K., Huang, J., Walcott, GP., Rogers, JM. Optical mapping of membrane potential and epicardial deformation in beating hearts. *Biophysics J.* **111** (2), 438-451 (2016).